Exosome-like Extracellular Vesicles from *MYCN*-amplified Neuroblastoma Cells Contain Oncogenic miRNAs

BJØRN HELGE HAUG[1], ØYVIND H. HALD[2], PETER UTNES[1], SARAH A. ROTH[2], CECILIE LØKKE[2], TROND FLÆGSTAD[1,2] and CHRISTER EINVIK[1,2]

[1]*Department of Pediatrics, University-Hospital of Northern-Norway (UNN), Tromsø, Norway;*
[2]*Pediatric Research Group, Department of Clinical Medicine, University of Tromsø, Tromsø, Norway*

Abstract. *Background: In recent years, evidence has accumulated indicating that both normal and cancer cells communicate via the release and delivery of macromolecules packed into extracellular membrane vesicles. Materials and Methods: We isolated nano-sized extracellular vesicles from MYCN-amplified neuroblastoma cell lines using ultracentrifugation and exosome precipitation (Exoquick) protocols. These vesicles were characterized by transmission electron microscopy (TEM), nanoparticle tracking analysis and western blotting. Exosomal miRNA profiles were obtained using a reverse transcription-polymerase chain reaction (RT-PCR) ready-to-use panel measuring a total of 742 miRNAs. Results: In this study, we showed that MYCN-amplified neuroblastoma cell lines secrete populations of miRNAs inside small exosome-like vesicular particles. These particles were shown to be taken-up by recipient cells. By profiling the miRNA content, we demonstrated high expression of a group of established oncomirs in exosomes from two MYCN-amplified neuroblastoma cell lines. Despite the fact that other studies have demonstrated the ability of exosomal miRNAs both to repress mRNA targets and to stimulate Toll-like receptor-8 (TLR8) signaling in recipient cells, we did not observe these effects with exosomes from MYCN-amplified neuroblastoma cells. However, functional enrichment analysis reveals that mRNA targets of highly expressed exosomal miRNAs are associated with a range of cellular and molecular functions related to cell growth and cell death. Conclusion: MYCN-amplified neuroblastoma cell lines secrete exosome-like particles containing oncogenic miRNAs. This work showed for the first time that neuroblastoma cells secrete exosome-like particles containing miRNAs with potential roles in cancer progression. These findings indicate a new way for MYCN-amplified neuroblastoma cells to interact with the tumor environment.*

Correspondence to: Christer Einvik, Department of Pediatrics, University-Hospital of Northern-Norway, 9037 Tromsø, Norway, Tel: +47 77669726, e-mail: christer.einvik@uit.no

Key Words: Exosome, neuroblastoma, microRNA, miRNA.

Neuroblastoma is the most common solid tumor in children and comprises 7% of pediatric cancers. It has a clinical behavior ranging from spontaneous regression to progressive and fatal disease resistant to currently known treatments (1). In order to develop more effective treatments, a broader knowledge of neuroblastoma pathogenesis and tumor biology is needed. One of the most important prognostic factors in neuroblastoma is amplification of the *MYCN* oncogene, present in 20% of cases (1, 2). *MYCN* encodes a transcription factor (N-Myc), which contributes to a malignant phenotype through transcriptional regulation of several genes (3).

Micro-RNAs (miRNAs) are a group of small, non-coding RNAs of great importance in normal gene regulation. Aberrant miRNA expression patterns have been linked to development of many diseases, including cancer. These molecules function primarily by post-transcriptionally down-regulating gene expression by binding to the 3' untranslated region (UTR) of messenger-RNAs (mRNAs), either by inhibiting their translation or through facilitating mRNA degradation (4). *MYCN* has been demonstrated to both increase and decrease the expression of oncogenic and tumor suppressive miRNAs, respectively. Several studies have investigated the role of *MYCN* in regulating miRNAs using RNAi-based approaches in *MYCN*-amplified neuroblastoma cell lines (5, 6). Other studies have used experimental over-expression of *MYCN* as a system for differential profiling of miRNAs (7-9). While different studies suggest that *MYCN* primarily functions as a suppressor of miRNA expression, it can also trans-activate the 17-92, 106a-363, 106b-25 clusters, as well as mir-9 and mir-421 through direct promoter binding (10).

Exosomes are nano-sized extracellular membrane vesicles containing several RNA species, including mRNAs and miRNAs, as well as proteins and DNA (11). Recent studies revealed that these biological macromolecules can function in intercellular communication through exosomal trafficking

0250-7005/2015 $2.00+.40

from immune cells, fibroblast and cancer cells to a range of different recipient cells (12). Exosomes originate by intraluminal budding in endosomes to form multivesicular bodies and are further transported to the cell membrane where they are released extracellularly (13). MiRNAs transported in exosomes are protected against degradation by RNases in the extracellular space and in the circulation. Exosomal miRNAs have been demonstrated not only to function through classical negative gene regulation by binding to mRNAs 3'UTR but also through stimulation of the Toll-like receptor 8 (TLR8) in humans and TLR7 in mice (14). This receptor is known to activate nuclear factor-κB (NF-kB) signaling in response to pathogen-associated RNA sequences (15). Recent investigations suggest that miRNAs, to a greater extent, allocate to multivesicular bodies with subsequent extracellular secretion when intracellular target-transcripts are scarce. In an abundance of target transcripts, miRNAs tend to favor sites associated with intracellular gene silencing (16).

Cancer cell-derived exosomes can modulate a diverse array of processes, including angiogenesis (17-19), anti-tumor immune responses (11) and metastatic potential (20-22). On the other hand, non-cancer cell-derived exosomes can also act by promoting growth inhibition of malignant cells (23).

The aim of the present study was to investigate whether miRNA-containing exosomes are secreted from *MYCN*-amplified neuroblastoma cells. We also wanted to test if exosomes could function as intercellular players in tumorigenesis by affecting gene expression in recipient cells.

In the present study, we utilize an improved protocol for culturing cells, which yield large amounts of exosomes (24). The miRNA content of exosome-like particles from two *MYCN*-amplified neuroblastoma cell lines was profiled and validated. The potency of exosomes to associate with different recipient cells and regulate target seed sequences or stimulate TLR8 signaling within recipient cells was investigated. Finally, we performed functional enrichment analyses on targets of highly expressed exosomal miRNAs. Our results indicate that exosomes derived from *MYCN*-amplified neuroblastoma cells may have important roles in tumor development.

Materials and Methods

Cell culture. All cells were cultured at 37˚C and 5% CO_2. The *MYCN*-amplified Kelly (ECACC, Porton Down, Salisbury, UK) and SK-N-BE(2)-C (kindly provided by Dr John Inge Johnsen, Karolinska Institutet, Stockholm, Sweden) neuroblastoma cell lines, as well as the non *MYCN*-amplified SK-N-AS (ATCC, Manassas, VA, USA) cell line were cultured in Roswell Park Memorial Institute medium (RPMI)-1640 containing L-glutamine and non-essential amino acids (Sigma-Aldrich, St. Luis, MO, USA). Similarly, HEK-293T (ATCC) cells were cultured in Dulbecco's modified Eagle's medium (DMEM; Sigma-Aldrich). The medium was supplemented with 10% fetal bovine serum (FBS). HEKblue-TLR8 cells (InvivoGen, San Diego, USA), stably expressing TLR8 and a reporter construct responsive to activator protein 1 (AP-1) and NF-kB activation as a readout for TLR8 stimulation, were cultured in high-glucose DMEM supplemented with 10% heat-inactivated FBS. Commercially provided HUVEC cells pooled from donors in accredited institutions (Life technologies, Carlsbad, CA, USA) were grown in medium-200 with low serum growth supplement (LSGS) (Life technologies). Consent for use of the cells in research applications was obtained from next of kin (25). Cells were split and subcultured before confluency.

The identity of the neuroblastoma cell lines used in this study was verified by short tandem repeat (STR) analysis at Center of Forensic Genetics, University of Tromsø, Tromsø, Norway. All cells used in this study were tested for mycoplasma contamination.

Isolation of exosomes. Exosome-depleted FBS was prepared by centrifugation at 4˚C over night at 170,000 ×g, followed by sterile filtration using 0.2 μm filters (Millipore Corporation, Billerica, MA 01821, USA). Exosome-free media (EFM) was prepared by addition of 10% exosome-depleted serum to RPMI-1640.

SK-N-BE(2)-C and Kelly cells were grown in Celline Adhere 1000 bioreactors (CLAD 1000) (Sigma-Aldrich) as previously described (24). The flasks have a small compartment for cells and a large compartment for media. A 10-kDa semi-permeable membrane that retains cells, exosomes and larger proteins, but allows exchange of nutrients and waste products, separates the two compartments. During exosome production, the medium compartment contained 500 ml complete RPMI-1640 and the cell compartment 15 ml EFM. Media from the cell compartment was collected for exosome isolation once a week. The compartment was then flushed vigorously 4 times using sterile 1× PBS, removing floating cells and other debris, before addition of fresh growth media to both compartments. After 4 isolations, adherent cells were trypsinized and checked for viability using PBS/0.4% Trypan blue staining. Exosomes were isolated by ultracentrifugation according to previously described protocols (26). Briefly, conditioned media was centrifuged at 200×g for 10 minutes, 2,000×g for 20 minutes, 10,000×g for 30 minutes and 110,000×g for 70 minutes to remove cells, debris and microvesicles, respectively. Unconditioned exosome-free media (EFM) was treated in parallel as a negative control. The amounts of exosomes isolated were measured using the Bio-Rad DC protein assay (Bio-Rad, Hercules, CA, USA) and stored at –80˚C or directly used in experiments.

Western blotting. Cells and exosomes were lysed in RIPA buffer (50mM Tris HCl, pH 8, 150 mM NaCl, 1% NP-40, 0.5% sodium deoxycholate, 0.1% SDS) supplemented with protease inhibitor cocktail (Roche Applied Science, Indianapolis, IN, USA). Thirty μg proteins were separated on NuPAGE 4-12% Bis-Tris Gels (Life technologies). Proteins were transferred onto Immobilon-FL polyvinylidene difluoride (PVDF) membranes (Millipore Corp., Bedford, MA, USA), blocked for 1 hour at room temperature in Odyssey Blocking Buffer (LI-COR, Lincoln, NE, USA) before incubation at 4˚C overnight with the primary antibodies CD9 sc-13118, CD63 sc-5275, GAPDH sc-25778, N-MYC sc-53113 (Santa Cruz, Dallas, TX, USA), TSG101 ab83 (Abcam, Cambridge, UK), GRP78 G8918, Actin A2066 (Sigma-Aldrich). Secondary antibodies were goat anti-rabbit IRDye800CW (Rockland, Gilbertsville, PA, USA) and goat anti-mouse Alexa Fluor 680 (Life technologies). Antibody binding was detected using the Odyssey Infrared Imaging System (LI-COR).

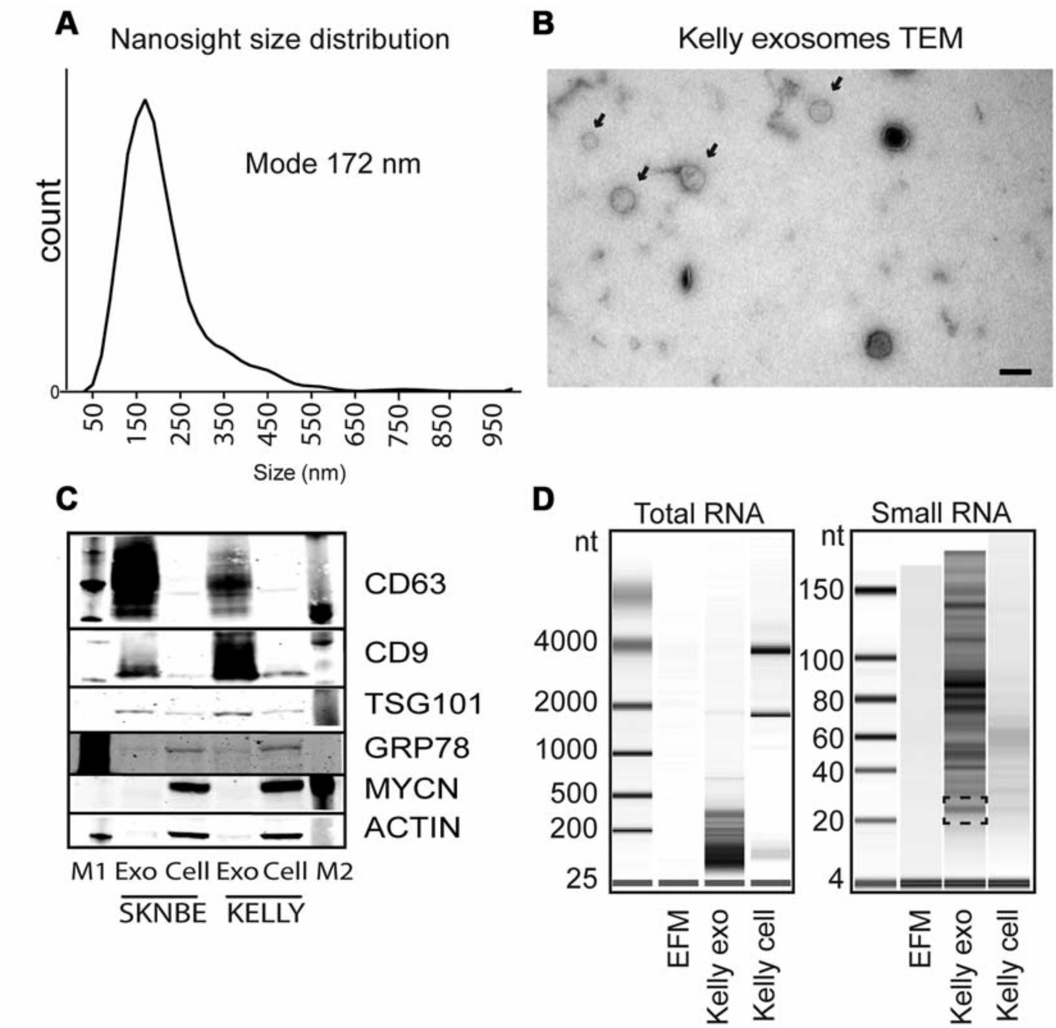

Figure 1. *Characterization of exosome isolates. A) Nanosight (nanoparticle-tracking analysis). Size distribution of isolated Kelly exosomes. B) Transmission electron microscopy (TEM) of PFA fixed exosomes on formvar grids at 80,000× magnification. The scale bar measures 100 nanometers. C) Western blotting of lysed exosomes and cells from the MYCN-amplified neuroblastoma cell lines SK-N-BE(2)–C and Kelly. The blot shows the exosomal markers CD63, CD9 and TSG101, as well as cellular GRP78, N-Myc and β-actin proteins. M1 and M2, markers. D) Analysis of total (left) and small (right) RNA fractions using the Agilent Bioanalyzer. The marker indicates nucleotide (nt) size.*

Characterization of the size and morphology of isolated particles using transmission electron microscopy (TEM) and Nanosight analysis. Exosome samples isolated by ultracentrifugation were washed, re-suspended in PBS and fixed in 2% paraformaldehyde (PFA). Subsequently, samples were loaded on formvar-coated electron microscopy (EM) grids. After washing, the samples were post-fixated in 1% gluteraldehyde. They were washed once more and, subsequently, stained in methyl cellulose-uranyl acetate for 10 min on ice. Grids were dried and examined using TEM at 80,000× magnification.

Isolated exosomes were further analyzed using the Nanosight LM10 system equipped with a 405 nm blue laser (Nanosight Ltd, Wiltshire, UK). The laser illuminated the isolated vesicles and the software recorded their movement under Brownian motion. Videos were subjected to nanoparticle tracking analysis using the provided software to acquire size distribution. All analysis parameters were kept constant within the experiments.

Profiling of exosomal miRNAs. Exosomal miRNA content was profiled from SK-N-BE(2)-C and Kelly cells. All miRNA assays were run in at least two biological isolates. Exosomes were isolated as specified and lysed in Qiazol reagent (Qiagen, Valencia, CA, USA). RNA was precipitated using isopropanol. RNA concentration was determined using the Qubit 2.0 RNA assay kit (Life technologies). The content and quality of the exosomal RNA was determined using the 2100 Bioanalyzer instrument with the small RNA and Eukaryote total RNA kits (Agilent technologies, Santa Clara, CA, USA). Forty ng total RNA was reverse transcribed using the miRCURY universal cDNA synthesis kit (Exiqon, Copenhagen, Denmark). RNA from exosomes and cells was profiled with the

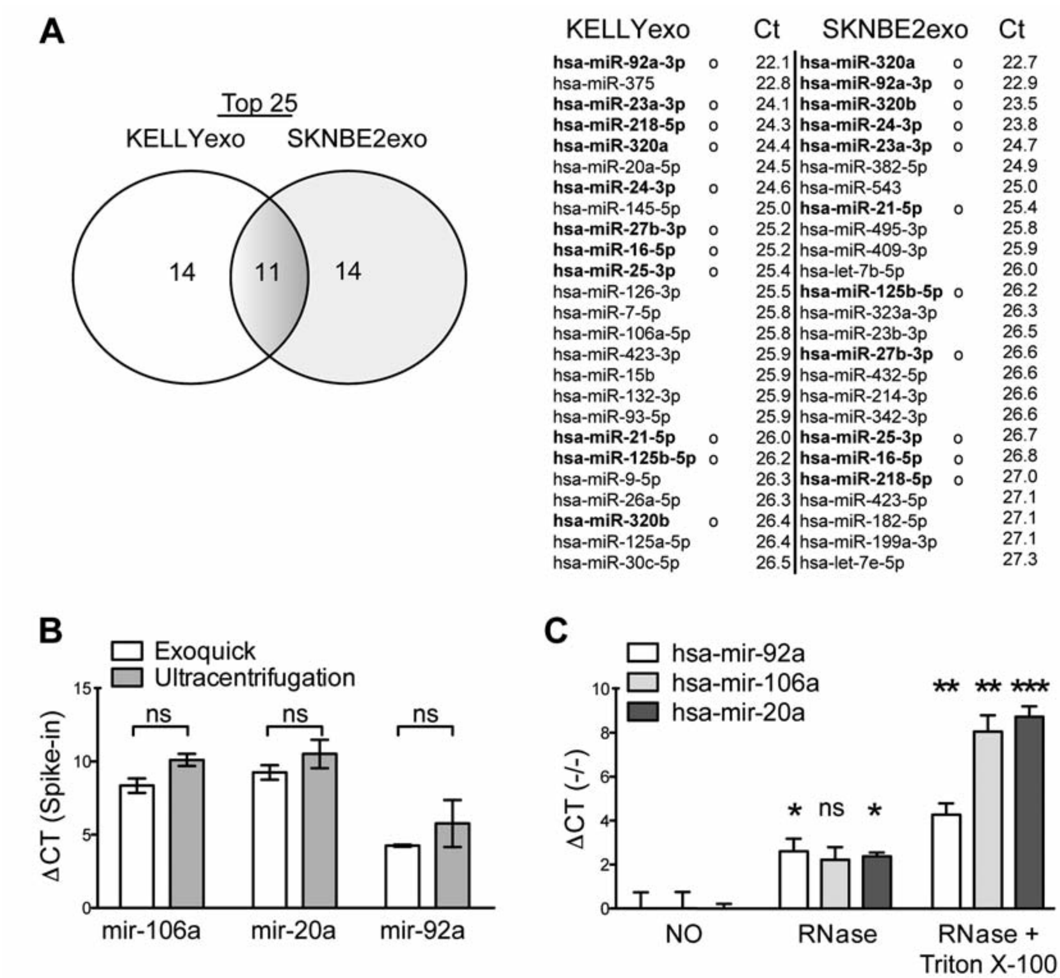

Figure 2. *miRNA expression in neuroblastoma exosome-like extracellular particles. A) Venn diagram of miRNAs expressed in exosomes from Kelly and SK-N-BE(2)-C cells (left). Average C_T values of miRNA assays in exosomal samples (right) from Kelly and SK-N-BE(2)-C cells. miRNAs commonly expressed among the top 25 in both cell lines constitute the overlapping fraction in the Venn diagram and are marked by a circle (o) in the table. B) The relative expression of three different miRNAs were measured in exosomal isolates from Kelly cell using two different isolation protocols (Exoquick and ultracentrifugation). $\Delta C_T = (C_{T\ miRNA\ assay} - C_{T\ spike\text{-}in})$. C) ΔC_T values in untreated samples (NO-set to 0), RNAse and RNase+Triton X-100 treated samples. Untreated samples were used as calibrators and set to zero. Increases in ΔC_T (compared to untreated samples-NO) indicate degradation in response to the treatment. Exosomes isolated from Kelly cells. Error bars indicate standard deviation. ns illustrates $^{*}p>0.05$, $^{**}p<0.05$, 0.01 and $^{***}p<0.001$.*

miRCURY qPCR panels 1+2 V2.M (Exiqon, Copenhagen, Denmark). ROX was included as a passive reference dye. Variations between plates were normalized using interplate calibrators and cycle threshold (C_T) values were, then, averaged between replicates. Unconditioned EFM was also profiled to determine background signal. C_T values <35 were considered detected. We included miRNA assays where the C_T value of the EFM control was >35, indicating no interfering bovine miRNAs. However, samples were included if (C_T EFM)–(C_T sample) >6.6, indicating a bovine background of less than 1% of the sample expression.

To further validate the origin of the isolated miRNAs, Kelly exosome preparations were obtained in parallel using both differential centrifugation and the Exoquick-TC polymer-based exosome precipitation solution. Exoquick isolation was performed according to the manufacturer's protocol (System Biosciences, Mountain View, CA, USA). Equal amounts of RNA were used as input and a spike in control was added before cDNA synthesis. The relation between the different isolation methods were compared and presented as ΔC_T normalized to the spike in ($C_{T\ spike\text{-}in}$-$C_{T\ miRNA}$). Individual miRNA primer assays (Exiqon) for mir-106a, mir-20a, mir-92a and a spike-in control were used to measure miRNA expression. Student's *t*-test statistics was used when comparing the isolation methods.

RNase A/Triton X-100 experiments. Equal amounts of exosomes were treated with 5 U/ml RNase A (Qiagen) in the presence or absence of 1% Triton X-100. Samples were incubated at 37˚C for 30 minutes followed by addition of Qiazol reagent. RNA was isolated and reverse transcribed as for profiling experiments. mir-

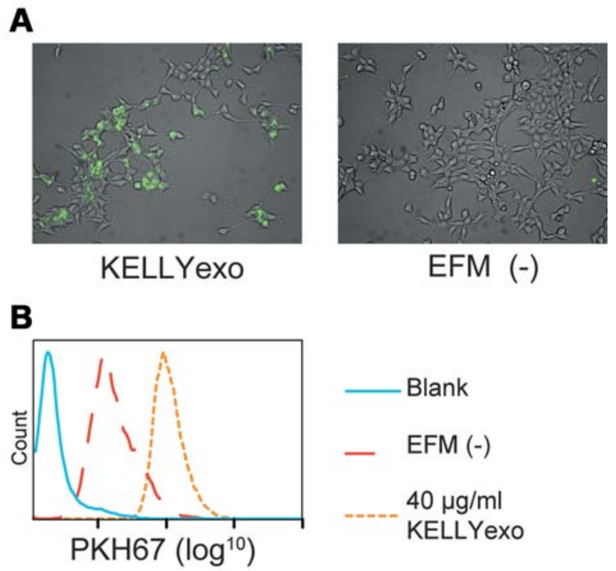

Figure 3. *Uptake of labeled exosomes in recipient cells. A) HEK-293T cells exposed to PKH67 (green)-labeled Kelly exosomes (KELLYexo) and EFM control. Pictures were taken at 400x magnification. B) Flow cytometry analysis of SK-N-AS cells exposed to fluorescent exosomes (KELLYexo) or controls (Blank=no treatment, EFM=exosome-free media).*

106a, mir-20a ,mir-92a were assayed as previously mentioned. Data are presented as ΔC_T ($C_{T\ sample}–C_{T\ untreated}$) using non-treated samples as calibrators. Statistical comparison of the treatments was performed using one-way ANOVA and Tukeys post-test.

Exosomal fluorescence staining and uptake. Kelly and SK-N-BE(2)-C-derived exosomes were isolated and washed in serum free RPMI-1640 to remove dye-binding proteins. The pelleted exosomes were resuspended in the provided buffer and stained with the lipophilic dye PKH67 (Sigma-Aldrich). Excess dye was inactivated using ten volumes exosome-depleted, serum containing media (EFM) and re-pelleted. Subsequently, the exosomes were washed twice in PBS, resuspended in unsubstituted medium, analyzed for protein concentration and added to recipient HEK-293T and SK-N-AS cells. Cells for microscopy and flow cytometry were exposed to 40 µg/ml exosomes. Twenty-four hours after addition, cells subjected to exosomes were examined using immunofluorescence microscopy and flow cytometry.

miRNA responsive luciferase assays. HEK-293T and SK-N-AS cells were used to measure uptake of functional miRNAs. For transfection, we used 1 µl/ml Lipofectamine 2000 (Life sciences) according to the manufacturer's instructions. Cells were co-transfected with the pMIR-report firefly-luciferase reporter vector (Promega, Madison, WI, USA) containing miRNA responsive seed sequences and the constitutively Renilla luciferase expressing vector pRL-TK (Promega). miRNA mimics targeting the relevant seed in the reporter vector and a scrambled control miRNA was used as positive and negative controls, respectively (Shanghai genepharma, Shanghai, China). The mir-92a insert was created by annealing the primers 5'-CTAGTATCTGG ACCAGGCTGTGGGTAGATGTGCAATAGAAATAGCTA-3'(sense) and 5'-AGCTTAGCTATTTCTATTGCACATCTACCCACAGCCTG GTCCAGATA-3' (antisense), corresponding to the mir-92a binding

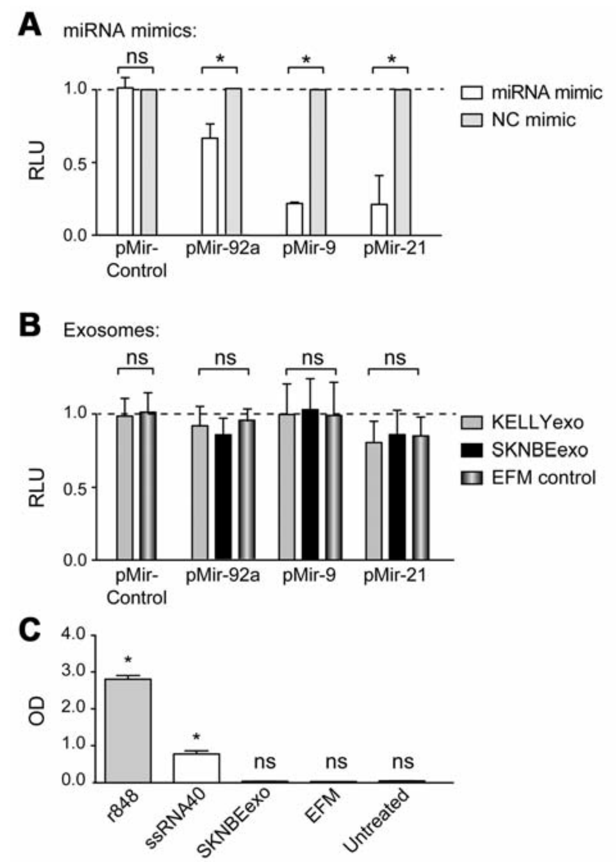

Figure 4. *Reporter activity for different exosomal miRNAs and ELISA for the mir-92 target DKK3 after treatment with exosomes. A) SK-N-AS cells expressing reporter constructs containing binding sites for no human miRNAs (pMir-Control), mir-92 (pMir-92a), mir-9 (pMir-9) and mir-21(pMir-21) were incubated with the corresponding miRNA mimics (40 pmols). Mimics without human targets (NC) (40 pmols) were used as negative controls. Luciferase activity was measured 24 h after transfection. RLU=relative luciferase units. B) Same as A, except 40 µg/ml isolated exosomes from Kelly (KELLYexo), SK-N-BE(2)-C (SKNBEexo) or control isolates (EFM control) were added to the transfected cells instead of miRNA mimics. C) Optical density (OD) measurements of culture media from HEKblue-TLR8 cells containing AP-1 and NF-kB responsive SEAP-expressing elements. Ccells were stimulated with positive controls r848 (5µg) or ssRNA40 (5µg), SK-N-BE(2)-C exosomes (SKNBEexo), EFM exosome control and untreated. Error bars indicate standard deviation. ns indicates $p>0.05$, $^{*}p<0.05$.*

site of the DKK3-3'UTR (27). The annealed primers were ligated into SpeI/HindIII-treated pMIR-Report vector to generate a mir-92a responsive firefly luciferase construct (pMIR-92a). Similarly, the pMIR-report-derived pMIR-9 (18) and pMIR-21-luc (kindly provided gift From Dr. Anders H. Lund, Copenhagen) vectors contain 3'UTR binding sites for mir-9 and mir-21 downstream of the firefly luciferase coding sequence. One-way ANOVA with Tukeys post-test was used when comparing the treatments.

TLR8 activation assay. One hundred thousand human HEKblue-TLR8 cells (Invivogen) were seeded in each 4 cm^2 well. Twenty-four hours

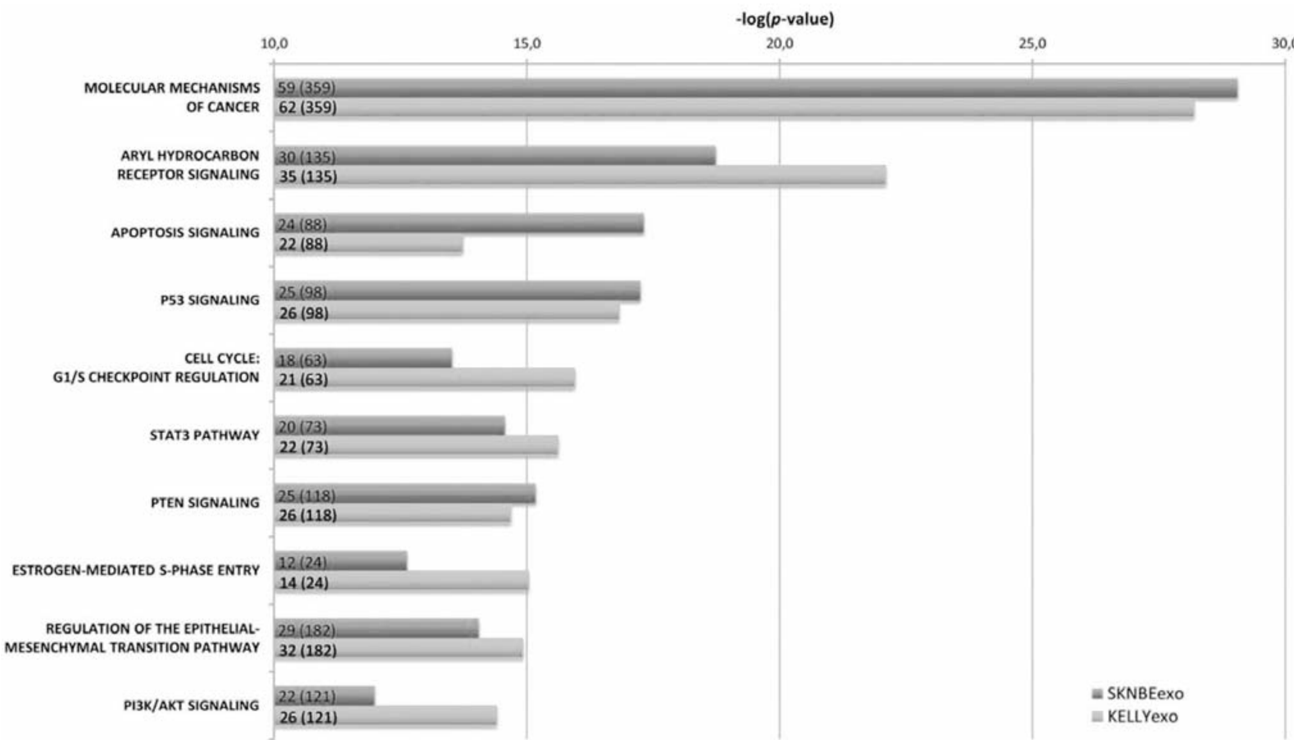

Figure 5. *Canonical pathways potentially affected by neuroblastoma exosomal miRNAs. Ingenuity pathway analysis (IPA) showing the canonical pathways that are most significantly affected by the target genes for the 25 highest expressed miRNAs isolated from SK-N-BE(2)-C and Kelly cells. The pathways are indicated on the y-axis. The x-axis indicates the significance score as negative log of p-values calculated using the Fisher's exact test. Numbers within the bars indicate identified predicted target genes to the pathway (of total genes in the pathway).*

after seeding, the cells were treated with exosomes (50 µg/ml) from SK-N-BE(2)-C cells . As positive controls, parallels were either transfected with 5 µg/ml of the viral ssRNA40 using 2 µL/ml Lipofectamine 2000 (Life sciences) or maintained in the presence of the molecular agonist R848 (5µg/ml). Twenty hours after treatment, the media was harvested and centrifuged at 21,100×g for 5 min to remove debris and secreted embryonic alkaline phosphatase (SEAP) levels in the supernatant was quantified using the QuantiBlue assay (InvivioGen, San Diego, CA 92121, USA). The data were statistically analyzed using one-way ANOVA with Tukeys post-test.

Functional enrichment analysis. Potential targets for the 25 highest expressed exosomal miRNAs were predicted using the Ingenuity Pathway Analysis (IPA) software (Ingenuity Systems, Redwood City, CA, USA). Here, three miRNA-mRNA interaction algorithms were used (TargetScan, TarBase and miRecords) and, to limit the total number of predicted mRNA targets, only the experimentally validated targets were selected for further analysis. The relationships among the predicted targets were also analyzed using IPA. Core analyses, filtered to use the Ingenuity Knowledge Base reference set with all human tissue and cell lines, were performed separately on each set of predicted miRNA targets. Finally, a comparison analysis was performed to identify common biological functions and canonical pathways predicted to be affected by exosomal miRNAs isolated from both SK-N-BE(2)-C and Kelly neuroblastoma cell lines.

Results

MYCN-amplified neuroblastoma-derived particles exhibit exosome-like characteristics. To determine if *MYCN*-amplified neuroblastoma cells secrete exosome-like vesicles, we isolated extracellular vesicles by a standard ultracentrifugation protocol from *in vitro* cultured Kelly and SK-N-BE(2)-C cells. Transmission electron microscopy and Nanosight size distribution analysis demonstrated a population of small circular particles between 50 to 350 nm, with a mode of 172 nm (Figure 1A and B). The EFM control media did not contain measurable levels of particles (data not shown). Western blot analysis demonstrated a striking enrichment of the tetraspanin exosomal markers CD63 and CD9. A more modest enrichment of another exosomal marker, TSG101, was seen. In contrast, the endoplasmic reticulum marker GRP78, the cytoskeletal component β-actin and the N-myc protein were almost exclusively detected in cellular lysates (Figure 1C). RNA composition analysis using a Bioanalyzer revealed that the exosome-like particles were highly enriched in small RNAs less than 300-400 nucleotides (nt). In contrast to cellular RNA, they also lacked cellular 18S and 28S ribosomal peaks, identifying the RNA composition

Table I. *IPA pathway analysis of neuroblastoma exosomal miRNA targets genes. Enriched functional categories as reported by IPA from the target genes for the 25 highest expressed miRNAs isolated from SK-N-BE(2)-C and Kelly cells. Number of molecules indicates potential miRNA target genes linked to each category. Range p-value shows the lowest and highest p-values from all under-categories.*

Category	Analyzed exosomal miRNAs	Molecules	Range *p*-values
Cellular	KELLYexo	226	1.6E-53-1.2E-07
development	SKNBEexo	185	8.6E-42-4.2E-07
Cellular growth	KELLYexo	242	1.6E-53-1.2E-07
and proliferation	SKNBEexo	206	8.6E-42-3.5E-07
Cell death	KELLYexo	227	2.8E-47-1.4E-07
and survival	SKNBEexo	191	1.2E-35-4.5E-07
Cellular	KELLYexo	161	5.6E-37-1.2E-07
movement	SKNBEexo	123	2.7E-26-3.9E-07
Cell cycle	KELLYexo	134	1.8E-32-1.6E-07
	SKNBEexo	123	4.2E-32-3.5E-07

as fundamentally different from their cells of origin (Figure 1 D, left panel). Analysis of small RNAs revealed a population of RNAs at about 23 nt, consistent with the expected size of miRNAs. In combination, these results confirm successful isolation of exosome-like particles from neuroblastoma cells.

MYCN-amplified neuroblastoma cells secrete exosome-like particles with a distinct miRNAs content. The miRNA content of exosome-like particles from *MYCN*-amplified neuroblastoma cell lines Kelly and SK-N-BE(2)-C was investigated using LNA-qPCR arrays. The top 25 expressed exosomal miRNAs isolated from both cell lines were compared and 11 of the exosomal miRNAs identified (mir-16, 125b, 21, 23a, 24, 25, 27b, 218, 320a, 320b and 92a) were common to both cell lines (Figure 2A, marked by circles).

To validate the origin of the assayed miRNAs, we compared the expression of three different miRNAs from Kelly exosomes using two different exosome isolation protocols. The Exoquick-TC and the ultracentrifugation exosome-isolates had almost identical expression of the three assayed miRNAs, mir-20a, mir-92a and mir-106b (Figure 2B). Furthermore, we investigated whether the secreted miRNAs were in fact resistant to RNase mediated degradation. Kelly-derived exosomes were treated with RNase in the presence or absence of Triton X-100 and the levels of mir-20a, mir-92a and mir-106b were quantified. A similar level of partial degradation across all samples was present when adding RNase A to the exosome suspension, while the degradation was further enhanced by addition of the detergent 1% Triton-×100 (Figure 2C).

Collectively, these results strongly suggest that the miRNAs investigated are indeed present within the isolated exosome-like particles.

Neuroblastoma exosomes associate with various recipient cells. To investigate if recipient cells take-up the isolated exosome-like particles, fluorescently labeled exosomes were added to cultured HEK-293T cells and tracked by microscopy. HEK-293T cells displayed significant uptake of labeled Kelly-derived exosomes after 24 h co-incubation (Figure 3A). Flow cytometry analysis of SK-N-AS (Figure 3B) cells similarly demonstrated exosome uptake, as measured by increased recipient cell fluorescence. Similar uptake in other cell lines tested, including HUVEC, SK-N-BE(2)-C and Kelly cell lines, was verified by both fluorescence microscopy and flow cytometry suggesting a wide range of potential recipient cells, including an autocrine uptake.

Exosomal miRNAs do not repress target gene expression or activate the endosomal TLR8 receptor in recipient cells. Mir-92a was the most highly expressed miRNA when considering exosomes from both cell lines examined. To investigate whether miRNA-containing exosomes could regulate established 3'UTR target seed-sequences in recipient cells, we transfected cells with miRNA sensing luciferase reporter vectors. Luciferase activity was significantly reduced after co-transfection with purified miRNA mimics (Figure 4A). However, we did not observe any significant differences in luciferase activity using mir-92a (pMIR-92a), mir-9 (pMIR-9) and mir-21 (pMIR-21-luc) responsive constructs when exposing SK-N-AS or HEK-293T cells to 40 µg/ml Kelly or SK-N-BE(2)-C exosomes. (Figure 4A).

Finally, we tested the recent finding that exosomal miRNAs may induce NF-kB activation through TLR8 activation. We stimulated HEKblue-TLR8 cells stably transfected with TLR8 and NF-kB/AP-1 SEAP reporter constructs with exosomes and controls. In contrast to the positive controls ssRNA40 and r848, SK-N-BE(2)-C exosomes did not give significant increases in SEAP levels compared to untreated cells (Figure 4C).

Functional enrichment analysis indicates that miRNAs from neuroblastoma exosomes are associated with signal pathways important for cell growth, survival and death. To evaluate the functions of miRNAs from neuroblastoma cell-derived exosomes, we used the IPA software to predict mRNA targets and performed a functional enrichment analysis on these predicted targets.

The 25 most abundantly expressed miRNAs from Kelly and SK-N-BE(2)-C exosomes were predicted to target 565 and 499 experimentally observed mRNAs, respectively. Furthermore, when these mRNAs were analyzed for functional categories, a range of cellular and molecular functions related to cell development, growth and death were identified (Table I).

When IPA was further used to analyze canonical pathways, we identified "Molecular Mechanisms of Cancer" (SKNBE2exo: $p=8.8\times10^{-30}$ n=59, KELLYexo: $p=6.4\times10^{-29}$ n=62), in addition to several well-characterized pathways like aryl hydrocarbon receptor- (SKNBE2exo: p=1.9×10^{-19} n=30, KELLYexo: p=8.0×10^{-23} n=35), apoptosis- (SKNBE2exo: p=4.9×10^{-18} n=24, KELLYexo: p=1.9×10^{-14} n=22), p53- (SKNBE2exo: p=5.7×10^{-18} n=25, KELLYexo: p=1.5×10^{-17} n=26), cell cycle (G1/S checkpoint)- (SKNBE2exo: p=3.0×10^{-14} n=18, KELLYexo: p=1.1×10^{-16} n=21), STAT3- (SKNBE2exo: p=2.7×10^{-15} n=20, KELLYexo: p=2.4×10^{-16} n=22) and PTEN- (SKNBE2exo: p=6.7×10^{-16} n=25, KELLYexo: p=2.1×10^{-15} n=26) signaling, to be the most significantly enriched pathways by the predicted miRNA targets (Figure 5). The full list of putative targets related to all significant pathways for both SK-N-BE(2)-c and Kelly exosomal miRNAs can be provided upon request.

Discussion

The aim of our study was to identify and profile exosomal miRNAs from *MYCN*-amplified neuroblastoma cells and to investigate their role in intercellular signaling by tumor cells.

The present data show that *MYCN*-amplified neuroblastoma cells secrete a population of small vesicles exhibiting the characteristics of exosomes. Enrichment of established exosomal markers like CD63, CD9 and TSG101, and absence of intracellular GRP78, β-actin and N-myc proteins provide further support for this conclusion. Previously, a full proteomic analysis of neuroblastoma-derived exosomes showed that, in addition to the exosomal markers, exosomes from neuroblastoma cells, also express proteins involved in defense response, cell differentiation, cell proliferation and regulation of other important biological processes, including the neuroblastoma specific marker GD2 disialoganglioside (28).

To further characterize the secreted vesicles, we performed nanoparticle tracking analysis using Nanosight and TEM and showed a size distribution of these particles similar to that found in exosome isolates (29-31). In addition, the enrichment in small RNAs and relatively low content of ribosomal RNA is also a previously described trait of exosomes. The RNA profiles identified in our samples match the findings in the two most in-depth descriptions of exosomal RNA content (32, 33). The authors of these articles used deep sequencing approaches and identified significant enrichments of small RNAs not restricted to and, in fact, not dominated by miRNAs. They also observed large amounts of Y-RNAs in the exosomes. We incidentally discovered high expression of a Y-RNA, previously believed to be a miRNA (mir-1979) (34) in exosomes from both Kelly and SK-N-BE(2)-C (average C_T of 22.2 and 21.1, respectively). The RNA distribution profiles of our exosome preparations clearly indicate larger populations of small RNAs in addition to the observed band corresponding to the size of miRNAs (20-25 nt). These different RNAs may have yet un-identified important functions. Deep sequencing approaches could be utilized in order to map for the complete transcriptome of these small vesicles.

By profiling the exosomal miRNA content, we identified a population of 11 miRNAs highly expressed from both screened cell lines. These miRNAs included several known oncogenic miRNAs. Recipient cells were associated with fluorescently stained exosomes after 24 h co-incubation, indicating uptake. However, luciferase reporter studies on mir-92a, mir-9 and mir-21 in cells exposed to exosomes did not yield any reduction in reporter activity in recipient cells. This was the case, even after addition of 40 μg/ml neuroblastoma exosomes, compared to 12.5 μg/ml exosomes in a comparable study (35).

Our experiments indicate that exosomal mir-92a, mir-9 and mir-21 do not have functional effects on established mRNA 3’UTR seed targets in the tested recipient cells, at least not without some co-stimulatory factor not yet identified. The recent finding that exosomal miRNAs can stimulate NF-kB signaling through binding and activating TLR8 in cellular endosomal compartments does not seem to be relevant with exosomes from *MYCN*-amplified neuroblastoma cells.

In order to obtain information regarding the potential role of the neuroblastoma-derived exosomal miRNAs, we performed a functional enrichment analysis using predicted mRNA target genes from the 25 highest expressed miRNAs. One of the highest scores was obtained for AHR signaling, shown to be involved in multiple aspects of cancer like survival, proliferation, differentiation, apoptosis, angiogenesis and invasion, reviewed in Feng *et al*. (36). Very recent data suggest that AHR is inversely correlated to *MYCN* expression in neuroblastoma tissue. Ectopic over-expression of AHR suppressed *MYCN* promoter activity resulting in down-regulation of *MYCN* expression, while AHR shRNA promoted the expression of *E2F1* and *MYCN* in neuroblastoma cells. AHR was suggested to be an important upstream regulator of *MYCN* (37).

The analyses further revealed that several canonical pathways known to be deregulated in most cancers are potentially impacted by the exosomal miRNAs. These include apoptosis-, p53- and G_1/S checkpoint regulation signaling. Aberrant STAT3 signaling is well-known to promote initiation and progression of several human cancers by either promotion of cell proliferation, survival, invasion, metastasis and angiogenesis, or inhibiting apoptosis (38). Recently, a critical role for STAT3 in metastatic drug resistant neuroblastoma was documented (39). Several reports during the last years have also established the importance of PTEN/PI3K/Akt signaling, including its relation to *MYCN*, in neuroblastoma survival, proliferation, invasion and angiogenesis (40-43).

The trophism and uptake of exosomes into different cells have been debated, but is believed to involve surface receptors (13). In contrast to other studies demonstrating direct seed interaction by exosomal miRNAs, we were not able to show any significant effects in recipient cells using our miRNA reporter assays. A recent study performed on immune cells demonstrated that exosome substitution alone was not enough for effects on miRNA reporters in recipient cells. Cell-to-cell contact and the subsequent formation of an immunological synapse were required for functional transmission of functionally active miRNA contents (44). Another recent study demonstrates that the lipid raft-associated Caveolin1 (CAV1) can inhibit uptake and function of exosomes by inhibiting ERK1/2 (29). It has also been demonstrated that phagocytic cells have a high uptake of exosomes, while the non-phagocytic cells only associate with exosomes without internalizing them (45). Considering these observations, it is not unlikely that the cell systems used in our studies lack the specific prerequisite conditions for exosomal miRNA function.

Conclusion

In this article, we present data demonstrating the secretion of exosome-like particles from two well-studied *MYCN*-amplified neuroblastoma cell lines. The exosomes are internalized into recipient cells and contain miRNAs with known oncogenic properties. Exosomal miRNAs may have roles in cell-to-cell signaling in neuroblastoma pathogenesis. However, our data do not support the theory that this happens through miRNA-seed sequence interaction or by activating the TLR8 receptor, as previously described in model systems of other cancers.

Acknowledgements

This work was supported by grants from the Northern-Norwegian Health Authorities (gene therapy program) and the Norwegian Cancer Society (Ragnvarda F. Sørvik and Håkon Starheims Foundation).

References

1 Maris JM, Hogarty MD, Bagatell R and Cohn SL: Neuroblastoma. Lancet *369*: 2106-2120, 2007.
2 Schwab M, Alitalo K, Klempnauer KH, Varmus HE, Bishop JM, Gilbert F, Brodeur G, Goldstein M and Trent J: Amplified DNA with limited homology to myc cellular oncogene is shared by human neuroblastoma cell lines and a neuroblastoma tumour. Nature *305*: 245-248, 1983.
3 Cheung L, Murray JE, Haber M and Norris MD: The MYCN Oncogene. *In*: Oncogene and Cancer-From Bench to Clinic. Siregar Y (ed.). InTech, pp 437-454, 2013.
4 Bartel DP: MicroRNAs: target recognition and regulatory functions. Cell *136*: 215-233, 2009.
5 Chen Y and Stallings RL: Differential patterns of microRNA expression in neuroblastoma are correlated with prognosis, differentiation, and apoptosis. Cancer Res *67*: 976-983, 2007.
6 Buechner J, Henriksen JR, Haug BH, Tømte E, Flaegstad T and Einvik C: Inhibition of mir-21, which is up-regulated during MYCN knockdown-mediated differentiation, does not prevent differentiation of neuroblastoma cells. Differentiation *81*: 25-34, 2011.
7 Lovén J, Zinin N, Wahlström T, Müller I, Brodin P, Fredlund E, Ribacke U, Pivarcsi A, Påhlman S and Henriksson M: MYCN-regulated microRNAs repress estrogen receptor-alpha (ESR1) expression and neuronal differentiation in human neuroblastoma. Proc Natl Acad Sci USA *107*: 1553-1558, 2010.
8 Shohet JM, Ghosh R, Coarfa C, Ludwig A, Benham AL, Chen Z, Patterson DM, Barbieri E, Mestdagh P, Sikorski DN, Milosavljevic A, Kim ES and Gunaratne PH: A genome-wide search for promoters that respond to increased MYCN reveals both new oncogenic and tumor suppressor microRNAs associated with aggressive neuroblastoma. Cancer Res *71*: 3841-3851, 2011.
9 Ma L, Young J, Prabhala H, Pan E, Mestdagh P, Muth D, Teruya-Feldstein J, Reinhardt F, Onder TT, Valastyan S, Westermann F, Speleman F, Vandesompele J and Weinberg R a: miR-9, a MYC/MYCN-activated microRNA, regulates E-cadherin and cancer metastasis. Nat Cell Biol *12*: 247-256, 2010.
10 Buechner J and Einvik C: N-myc and Noncoding RNAs in Neuroblastoma. Mol Cancer Res: 1243-1253, 2012.
11 Bobrie A, Colombo M, Raposo G and Théry C: Exosome secretion: molecular mechanisms and roles in immune responses. Traffic *12*: 1659-1668, 2011.
12 Valadi H, Ekström K, Bossios A, Sjöstrand M, Lee JJ and Lötvall JO: Exosome-mediated transfer of mRNAs and microRNAs is a novel mechanism of genetic exchange between cells. Nat Cell Biol *9*: 654-659, 2007.
13 Raposo G and Stoorvogel W: Extracellular vesicles: Exosomes, microvesicles, and friends. J Cell Biol *200*: 373-383, 2013.
14 Fabbri M, Paone A, Calore F, Galli R, Gaudio E, Santhanam R, Lovat F, Fadda P, Mao C, Nuovo GJ, Zanesi N, Crawford M, Ozer GH, Wernicke D, Alder H, Caligiuri MA, Nana-Sinkam P, Perrotti D and Croce CM: MicroRNAs bind to Toll-like receptors to induce prometastatic inflammatory response. Proc Natl Acad Sci USA *109*: E2110-2116, 2012.
15 Cervantes JL, Weinerman B, Basole C and Salazar JC: TLR8: the forgotten relative revindicated. Cell Mol Immunol 9: 434-438, 2012.
16 Squadrito ML, Baer C, Burdet F, Maderna C, Gilfillan GD, Lyle R, Ibberson M and De Palma M: Endogenous RNAs Modulate MicroRNA Sorting to Exosomes and Transfer to Acceptor Cells. Cell Rep: 1-15, 2014.
17 Nazarenko I, Rana S, Baumann A, McAlear J, Hellwig A, Trendelenburg M, Lochnit G, Preissner KT and Zöller M: Cell surface tetraspanin Tspan8 contributes to molecular pathways of exosome-induced endothelial cell activation. Cancer Res *70*: 1668-1678, 2010.
18 Zhuang G, Wu X, Jiang Z, Kasman I, Yao J, Guan Y, Oeh J, Modrusan Z, Bais C, Sampath D and Ferrara N: Tumour-secreted miR-9 promotes endothelial cell migration and angiogenesis by activating the JAK-STAT pathway. EMBO J: 1-11, 2012.
19 Umezu T, Ohyashiki K, Kuroda M and Ohyashiki JH: Leukemia cell to endothelial cell communication *via* exosomal miRNAs. Oncogene: 1-9, 2012.
20 Peinado H, Alečković M, Lavotshkin S, Matei I, Costa-Silva B, Moreno-Bueno G, Hergueta-Redondo M, Williams C, García-Santos G, Ghajar CM, Nitadori-Hoshino A, Hoffman C, Badal K, Garcia B a, Callahan MK, Yuan J, Martins VR, Skog J, Kaplan RN, Brady MS, Wolchok JD, Chapman PB, Kang Y, Bromberg J and Lyden D: Melanoma exosomes educate bone marrow progenitor cells toward a pro-metastatic phenotype through MET. Nat Med *18*: 883-891, 2012.

21 Luga V, Zhang L, Viloria-Petit AM, Ogunjimi AA, Inanlou MR, Chiu E, Buchanan M, Hosein AN, Basik M and Wrana JL: Exosomes mediate stromal mobilization of autocrine Wnt-PCP signaling in breast cancer cell migration. Cell *151*: 1542-1556, 2012.
22 Kogure T, Lin W-L, Yan IK, Braconi C and Patel T: Intercellular nanovesicle-mediated microRNA transfer: a mechanism of environmental modulation of hepatocellular cancer cell growth. Hepatology *54*: 1237-1248, 2011.
23 Kosaka N, Iguchi H, Yoshioka Y, Hagiwara K, Takeshita F and Ochiya T: Competitive interactions of cancer cells and normal cells *via* secretory microRNAs. J Biol Chem *287*: 1397-1405, 2012.
24 Mitchell JP, Court J, Mason MD, Tabi Z and Clayton A: Increased exosome production from tumour cell cultures using the Integra CELLine Culture System. J Immunol Methods *335*: 98-105, 2008.
25 Life Technologies: Certificate of analysis. 887799: 1, 2011. Available from: http://tools.lifetechnologies.com/Content/SFS/COAPDFs/2011/887799_C0155C.pdf.
26 Rani S, Brien KO, Kelleher FC, Corcoran C, Germano S, Radomski MW, Crown J and Driscoll LO: Isolation of Exosomes for Subsequent mRNA, MicroRNA, and Protein Profilin. *In*: Methods. O'Driscoll L (ed.). Totowa, NJ, Humana Press, pp 181-195, 2011.
27 Haug BH, Henriksen JR, Buechner J, Geerts D, Tømte E, Kogner P, Martinsson T, Flægstad T, Sveinbjørnsson B and Einvik C: MYCN-regulated miRNA-92 inhibits secretion of the tumor suppressor DICKKOPF-3 (DKK3) in neuroblastoma. Carcinogenesis *32*: 1005-1012, 2011.
28 Marimpietri D, Petretto A, Raffaghello L, Pezzolo A, Gagliani C, Tacchetti C, Mauri P, Melioli G and Pistoia V: Proteome profiling of neuroblastoma-derived exosomes reveal the expression of proteins potentially involved in tumor progression. PLoS One *8*: e75054, 2013.
29 Svensson KJ, Christianson HC, Wittrup A, Bourseau-Guilmain E, Lindqvist E, Svensson LM, Morgelin M and Belting M: Exosome uptake depends on ERK1/2-heat shock protein 27 signalling and lipid raft-mediated endocytosis negatively regulated by caveolin-1. J Biol Chem *288*: 17713-17724, 2013.
30 Garnier D, Magnus N, Lee TH, Bentley V, Meehan B, Milsom C, Montermini L, Kislinger T and Rak J: Cancer cells induced to express mesenchymal phenotype release exosome-like extracellular vesicles carrying tissue factor. J Biol Chem *287*: 43565-43572, 2012.
31 Kucharzewska P, Christianson HC, Welch JE, Svensson KJ, Fredlund E, Ringnér M, Mörgelin M, Bourseau-Guilmain E, Bengzon J and Belting M: Exosomes reflect the hypoxic status of glioma cells and mediate hypoxia-dependent activation of vascular cells during tumor development. Proc Natl Acad Sci USA *110*: 7312-7317, 2013.
32 Bellingham S a, Coleman BM and Hill AF: Small RNA deep sequencing reveals a distinct miRNA signature released in exosomes from prion-infected neuronal cells. Nucleic Acids Res *40*: 10937-10949, 2012.
33 Nolte-'t Hoen ENM, Buermans HPJ, Waasdorp M, Stoorvogel W, Wauben MHM and 't Hoen P a C: Deep sequencing of RNA from immune cell-derived vesicles uncovers the selective incorporation of small non-coding RNA biotypes with potential regulatory functions. Nucleic Acids Res *40*: 9272-9285, 2012.
34 Meiri E, Levy A, Benjamin H, Ben-David M, Cohen L, Dov A, Dromi N, Elyakim E, Yerushalmi N, Zion O, Lithwick-Yanai G and Sitbon E: Discovery of microRNAs and other small RNAs in solid tumors. Nucleic Acids Res *38*: 6234-6246, 2010.
35 Montecalvo A, Larregina AT, Shufesky WJ, Stolz DB, Sullivan MLG, Karlsson JM, Baty CJ, Gibson G a, Erdos G, Wang Z, Milosevic J, Tkacheva O a, Divito SJ, Jordan R, Lyons-Weiler J, Watkins SC and Morelli AE: Mechanism of transfer of functional microRNAs between mouse dendritic cells *via* exosomes. Blood *119*: 756-766, 2012.
36 Feng S, Cao Z and Wang X: Role of aryl hydrocarbon receptor in cancer. Biochim Biophys Acta *1836*: 197-210, 2013.
37 Wu P-Y, Liao Y-F, Juan H-F, Huang H-C, Wang B-J, Lu Y-L, Yu I-S, Shih Y-Y, Jeng Y-M, Hsu W-M and Lee H: Aryl hydrocarbon receptor downregulates MYCN expression and promotes cell differentiation of neuroblastoma. PLoS One *9*: e88795, 2014.
38 Siveen KS, Sikka S, Surana R, Dai X, Zhang J, Kumar AP, Tan BKH, Sethi G and Bishayee A: Targeting the STAT3 signaling pathway in cancer: role of synthetic and natural inhibitors. Biochim Biophys Acta *1845*: 136-154, 2014.
39 Ara T, Nakata R, Sheard MA, Shimada H, Buettner R, Groshen SG, Ji L, Yu H, Jove R, Seeger RC and DeClerck YA: Critical role of STAT3 in IL-6-mediated drug resistance in human neuroblastoma. Cancer Res *73*: 3852-3864, 2013.
40 Peirce SK, Findley HW, Prince C, Dasgupta A, Cooper T and Durden DL: The PI-3 kinase-Akt-MDM2-survivin signaling axis in high-risk neuroblastoma: a target for PI-3 kinase inhibitor intervention. Cancer Chemother Pharmacol *68*: 325-335, 2011.
41 Hogarty MD and Maris JM: PI3King on MYCN to improve neuroblastoma therapeutics. Cancer Cell *21*: 145-147, 2012.
42 Megison ML, Gillory LA and Beierle EA: Cell survival signaling in neuroblastoma. Anticancer Agents Med Chem *13*: 563-575, 2013.
43 Qiao J, Lee S, Paul P, Qiao L, Taylor CJ, Schlegel C, Colon NC and Chung DH: Akt2 regulates metastatic potential in neuroblastoma. PLoS One *8*: e56382, 2013.
44 Mittelbrunn M, Gutiérrez-Vázquez C, Villarroya-Beltri C, González S, Sánchez-Cabo F, González MÁ, Bernad A and Sánchez-Madrid F: Unidirectional transfer of microRNA-loaded exosomes from T cells to antigen-presenting cells. Nat Commun *2*: 282, 2011.
45 Feng D, Zhao W-L, Ye Y-Y, Bai X-C, Liu R-Q, Chang L-F, Zhou Q and Sui S-F: Cellular internalization of exosomes occurs through phagocytosis. Traffic *11*: 675-687, 2010.

Received January 26, 2015
Revised February 6, 2015
Accepted February 9, 2015